University of Reading

Experimental validation of the recovery effect in batteries for wearable sensors and healthcare devices discovering the existence of hidden time constants

Article

Published Version

Creative Commons: Attribution 3.0 (CC-BY)

Open Access

Arora, H., Sherratt, R. S. ORCID: https://orcid.org/0000-0001-7899-4445, Janko, B. and Harwin, W. ORCID: https://orcid.org/0000-0002-3928-3381 (2017) Experimental validation of the recovery effect in batteries for wearable sensors and healthcare devices discovering the existence of hidden time constants. The Journal of Engineering, 2017 (10). pp. 548-556. ISSN 2051-3305 doi: 10.1049/joe.2017.0303 Available at https://centaur.reading.ac.uk/72519/

It is advisable to refer to the publisher's version if you intend to cite from the work. See Guidance on citing.

To link to this article DOI: http://dx.doi.org/10.1049/joe.2017.0303

Publisher: Institution of Engineering and Technology

All outputs in CentAUR are protected by Intellectual Property Rights law, including copyright law. Copyright and IPR is retained by the creators or other copyright holders. Terms and conditions for use of this material are defined in

the End User Agreement.

www.reading.ac.uk/centaur

CentAUR

Central Archive at the University of Reading

Reading's research outputs online

Experimental validation of the recovery effect in batteries for wearable sensors and healthcare devices discovering the existence of hidden time constants

Harneet Arora, Robert Simon Sherratt, Balazs Janko, William Harwin

Department of Biomedical Engineering, University of Reading, Reading RG6 6AY, UK
E-mail: sherratt@ieee.org

Published in *The Journal of Engineering*; Received on 17th July 2017; Accepted on 17th September 2017

Abstract: Wearable sensors and healthcare devices use small lightweight batteries to power their operations of monitoring and tracking. It becomes absolutely vital to effectively utilise all the available battery charge for device longevity between charges. The electrochemical recovery effect enables the extraction of more power from the battery when implementing idle times in between use cycles, and has been used to develop various power management techniques. However, there is no evidence concerning the actual increase in available power that can be attained using the recovery effect. Also, this property cannot be generalised on all the battery chemistries since it is an innate phenomenon, relying on the anode/cathode material. Indeed recent developments suggest that recovery effect does not exist at all. Experimental results to verify the presence and level of the recovery effect in commonly used battery chemistries in wearable sensors and healthcare devices are presented. The results have revealed that the recovery effect significantly does exist in certain batteries, and importantly the authors show that it is also comprised of two different time constants. This novel finding has important implications for the development of power management techniques that utilise the recovery effect with application in a large range of battery devices.

1 Introduction

Wearable sensor devices have gained wide acceptance in healthcare monitoring and diagnostic applications. These devices allow ubiquitous sensing of the physiological, biochemical and motion-related parameters of the body without any physical assistance from medical professionals. The information collected by the sensors can be relayed to a central hub from where it can be accessed by their individual doctors, carers and family members. However, these devices face a number of challenges which need to be addressed for them to provide an efficient and reliable service. One such key issue is the ultra-low power, long-term wireless connectivity enabling wearables to be able to connect to the central hub at all times and vice versa. The ability to maintain a connection or perform processing largely depends on the amount of energy the device has to expend on this process. The device generally derives power from its battery power source. The amount of power available is constrained by the size and weight of the wearable. As such it is desirable to make optimal use of the available power source so as to prolong the time between required recharge cycles or to replace a non-rechargeable battery [1].

A number of strategies for the effective management of the power available in batteries have been proposed that allow them to last longer than usual. These techniques generally involve enhancement, modification or development of protocols either based on utilising the inherent characteristics of the source or by simply managing the application scenarios. The intuitive phenomenon which has been used so far is the recovery effect. This phenomenon increases the useful power of the source when it is allowed to rest in between discharge cycles [2]. Fig. 1 depicts this concept. It can be realised that the source lasts longer in the case of intermittent discharge in comparison with the continuous discharge. Intermittent discharge is created when the wearable is periodically put to sleep as opposed to being active, thus allowing the battery to self-recover.

The recovery effect has been widely used for modelling battery behaviour and several protocols have also been designed. However, only a limited set of experimental work is available to determine the presence and amount of recovery gain with regard to different battery chemistries. Surprisingly, most of the research to date has been based on the findings of just a small set of experiments. These experiments were conducted on specific chemistries and size of the batteries, and hence do not generalise to a battery of every size and shape. In contrast to the literature reporting the benefits and utilisation of recovery effect, it has been recently stated that recovery effect is just an illusion and has been wrongly used in all the literature stating its benefit [4]. It has been suggested that the parameters used for identifying and measuring the recovery effect are inappropriate. Much of the literature has not given an indication of the potential charge gain when implementing the recovery effect. As such the existence of the recovery effect has become controversial, yet battery-powered devices are ubiquitous and have a huge growing market, thus extending the required time between charges of battery devices can have a significant impact.

The present paper has been carried out to understand and demonstrate whether the recovery effect is a reality or an illusion. This paper has considered the typical chemistries used in wearable devices and revealed the chemistries that do offer the recovery effect. Furthermore, a novel contribution of this work is that, for the first time, the recovery effect has been shown to be comprised of two time constants: one short and one long. Therefore, battery management systems will need to take both time constants into consideration for maximum battery power extraction. Multiple sets of experiments on commonly used battery chemistries have been conducted offering authentic and reliable results. This work aims to give a perspective toward the parameters that should be used for analysing the recovery effect. A novel battery discharge system with constant-current drain capabilities has been designed for this purpose. Our discharge circuit is the first to test for the recovery effect while still drawing a small sleep current from the battery under test, in order to better model batteries deployed in actual devices. Also, the discharge timings and discharge current values have been chosen such that they can be related to the actual discharge characteristics of typical wearable devices.

This paper has been divided into ten sections. Section 2 describes the battery structure and a chemical description of the recovery effect. Section 3 discusses the battery requirements for intermittent discharge. Section 4 forms the primary literature survey. Section 5 presents the specific motivation for this research. Section 6 details the experimental setup and the scenarios used for the experiments.

doi: 10.1049/joe.2017.0303
This is an open access article published by the IET under the Creative Commons Attribution License (http://creativecommons.org/licenses/by/3.0/)

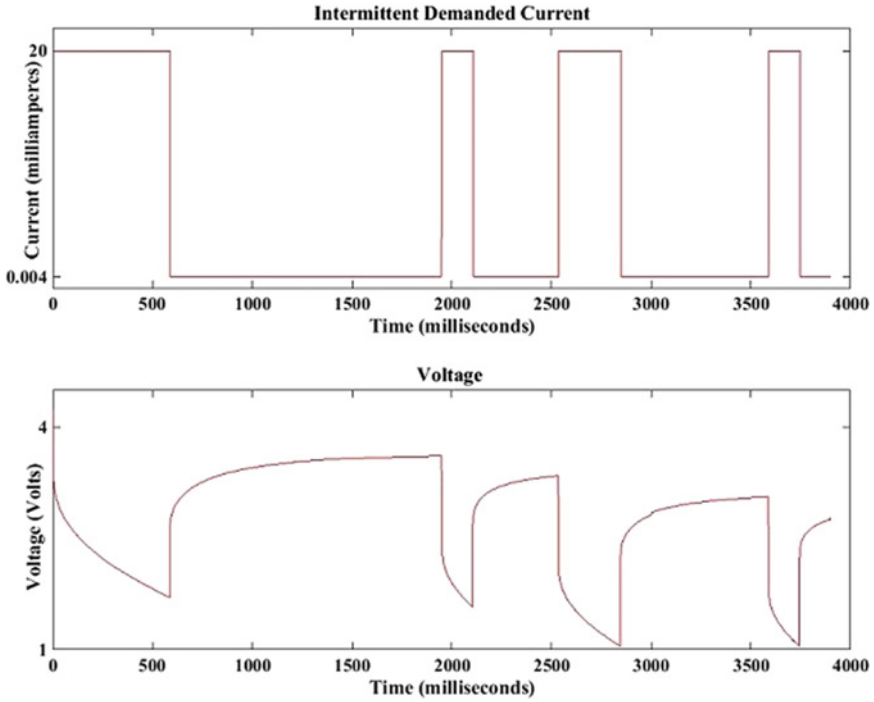

Fig. 1 *Concept of recovery effect in the case of intermittent discharge [3]*

Section 7 presents the results obtained followed by a discussion in Section 8, conclusions in Section 9 and future work in Section 10.

2 Chemical description of the recovery effect

A battery converts the chemical energy stored in electrochemical cells to electrical energy [5]. A cell comprises of an anode and a cathode separated by an electrolyte. When a load is connected to the cell, an oxidation reaction takes place at the anode whereby it loses electrons to the cathode via the external load. These electrons get accepted at the cathode leading to a reduction reaction. In a fully charged state, the electroactive species on both the anode and cathode are homogeneously distributed on the electrode–electrolyte interface [6, 7]. During discharge, the species near the electrode are consumed first and are continuously replaced by others that are further from the electrode. The rate at which this replacement takes place depends on the diffusion constant. If the battery is subjected to long periods of continuous discharge, then the electroactive species at the further end do not get enough time to travel toward the electrode resulting in the battery appearing to have been quickly depleted without all the species actually being consumed. However, if some time is given to the species to travel toward the electrode in between discharges, then additional species can undergo redox reaction and hence allow the battery to last longer [8]. This process of having idle time in between discharges to have more species participating in redox reaction is termed the recovery effect. Since the diffusion rate and the distance to travel toward the electrode play a significant role in the recovery process, it can be realised that batteries with different chemistries, shapes and sizes will show different amounts of recovery. Fig. 1 shows a typical battery recovery effect due to a high-current demand and a sleep current demand of a typical wearable device. As can be seen, when the device is in sleep mode then the battery terminal voltage recovers over time with species movement.

3 Battery requirements for intermittent discharge

The recovery process requires a battery to undergo intermittent discharge of high-current values followed by periods of low or no current (termed idle current). As such the battery should not only be able to withstand high pulses of current but should also provide a high proportion of energy pertaining to low current. Also, the rate of response when the switching between high and low currents happens should be very fast, i.e. the voltage should not take a long time to get to a steady state. In addition to this, the inductive effects at high frequencies should not cause waveform distortion [9].

4 Related work

Several experiments have previously been conducted to analyse the effect of intermittent discharge on different battery chemistries. Some of these studies were not aimed at identifying the ability of a battery to recover charge but were rather performed with an intention of analysing a battery's tolerance for high-current pulsed discharge or for understanding the chemical effect that takes place on the material comprising the battery during the rest periods. Table 1 summarises the details of these previous works.

Fuller *et al.* [12] conducted experiments to understand the redistribution of material that takes place when rest times are allowed in between charging and discharging of the cells. An off-the-shelf mobile phone cell battery and a custom-made lithium (Li) foil manganese dioxide cell were analysed for their behaviour. The solution phase concentration and state of charge (SOC) at each electrode along with the cell potential were the parameters considered for analysis. The custom-made cell was put to discharge with a current density of 0.7 mA/cm^2 for 3 h and then relaxed for 1 h with no discharge current. It was observed that when the current was interrupted in order to put the cell to rest, the front of the positive electrode was at lower potential and its back was at higher potential while it was the opposite case for the negative electrode, with its back being at a higher potential and front at a lower potential. This happened due to the sudden disruption of the discharge cycle. The difference in the potential between the front and back of the electrode leads to the flow of active material from the surface of high potential to low potential. The state of the charge of the electrode was a non-uniform function at the beginning of the relaxation period and later transformed into a uniform function. For the mobile phone cell battery, the discharge current of 1.9 A for

This is an open access article published by the IET under the Creative Commons Attribution License (http://creativecommons.org/licenses/by/3.0/)

doi: 10.1049/joe.2017.0303

Table 1 Details of previous relevant experimental studies conducted on batteries

Study	Battery chemistry	Off the shelf	Battery capacity/area	Active current/ current density	Active time, s	Sleep time, s	Parameters
[10]	alkaline,	yes	1800 mAh	1.5 A	900,	900,	total run time,
	NiCd,	yes	2000 mAh		1800	1800	battery temperature
	Ni–MH,	yes	4500 mAh				
	Li-ion	yes	1400 mAh				
[11]	lead acid,	no	5 cm^2	>=10 A/cm^2	0.003	0.022	cell potential,
	bipolar cell	no	20 cm^2				current density,
							power, W/cm^2
[12]	Li foil cell,	no	1 Ah	0.7 mA/cm^2	10,800,	3600	SOC at electrodes,
	Sony Li-ion phone cell	yes		1.9 A	960	3600	cell potential,
							solution phase concentration
[9]	TMF lead acid	yes	1.2 Ah	100 A	1	1	total run time
[13]	carbon/$LiNiO_2$,	no	10 cm^2	10–50 mA/cm^2	0.01	0.05	cell voltage,
	graphite/Li_nNiO_2	no					number of pulses
[4]	alkaline,	yes	1200 mAh	40 mW	50, 5, 0.5	50, 5, 0.5	voltage, power
	Ni–MH,	yes	730 mAh	40 mW			energy, Wh
	Li-ion	yes	400 mAh	80 mW			
[14]	Samsung	yes	2.6 Ah	nominal capacity/20	36,000	12, 7200	discharge capacity,
	ICR-18650-26F,	yes	1.1 Ah				break durations,
	A123 systems						SOC,
	APR-18650-M1A						discharge time
[15]	$LiFePO_4$,	no	5 Ah	0.5, 2 C	varying SOC states	20	diffusion time constant
	$LiMn_2O_4$	no	6 Ah				

TMF: thin metal film; Li-ion: lithium-ion; NiCd: nickel cadmium; Ni–MH: nickel-metal Hydride; and H: hours; Wh: watt hours.

16 min followed by a period of no current of 1 h was used. The cell potential in this case first rises instantly as soon as the load was disconnected and then increased gradually with the decrease in concentration over-potential and the relaxation of the concentration gradient.

Other battery studies [9, 11, 13] were aimed at analysing their custom-made batteries for their ability to handle the pulsed discharge with high discharge current. Nelson *et al.* [9] tested a thin metal film (TMF) battery to obtain its discharging and re-charging capabilities including pulsed discharge. The battery was subjected to an active current of 100 A for 1 s followed by a rest period with no current for the same time. An increase of 13.63% in the total run time was observed with pulsed discharge in comparison with the continuous discharge. Lafollette [11] tested batteries under high pulse currents. The current density chosen during the active cycle was at or above 10 A/cm^2. The discharge period was 3 ms followed by 22 ms rest period. Current density, cell potential and power were parameters used for analysis and it was observed that the behaviours of these batteries were nearly the same under both the continuous and intermittent discharge conditions. Similarly, Lee *et al.* [13] analysed the behaviour of Li nickel dioxide ($LiNiO_2$) cathode material under intermittent discharge with a carbon and graphite anode. The carbon/$LiNiO_2$ cell was pulse discharged at 10 mA/cm^2 for 10 ms followed by a rest period of 50 ms while graphite/$LiNiO_2$ was discharged with 10–40 mA/cm^2. Both the cells showed excellent capacity utilisation.

Another set of studies which have been carried out with the aim of analysing their ability to show recovery effect have been previously described [4, 10]. Narayanaswamy *et al.* [4] placed alkaline, Ni–metal hydride (MH) and Li-ion batteries under constant power discharge for 0.5, 5 and 50 s followed by a rest time for the same period. The battery voltage, power and energy were analysed. The authors claimed that the recovery effect does not incur any gain in energy but rather the continuous discharge delivers the same average power compared with intermittent discharge due to the reduced peak power. Castillo *et al.* [10] tested D-sized alkaline, Ni cadmium (Cd), Ni–MH and Li-ion batteries with capacity in the range of 1400–4500 mAh for two rest durations of 15 and 30 min. Their experiments recorded the total run time and battery voltage. The results showed that alkaline, NiCd and Ni–MH have a tendency to recover charge while there was no effect observed in Li-ion.

Recently, a couple more studies have been conducted to understand the influence of relaxation time on battery parameters [14, 16]. Reichert *et al.* [14] studied commercial Li-ion and found that there was no change in the battery discharge time when incorporating rest times. It was however highlighted that frequent shorter rest periods have a worst effect on ageing in comparison with the fewer but long sleep intervals. Devarakonda and Hu [16] reported research on customised Li-based single cells to explore how diffusion time constant varies with the open-circuit time.

5 Motivation

All of the aforementioned studies tested batteries for their behaviour under intermittent discharge but have not clearly analysed the existence of the recovery effect and exactly what, if any, benefits can be achieved when implementing intermittent discharge. Also, in all previous studies in the literature, the sleep current was considered to be zero, whereas in real practical devices, even when the device is put to sleep, there is still some sleep current. Therefore, to analyse the performance of batteries in realistic situations, the sleep current should be taken into consideration. Furthermore, as previously stated by Narayanaswamy *et al.* [4] the intermittent discharge profile of the battery should be compared with the continuous discharge which has the same average power of that of the intermittent discharge. It is claimed that this is a fair comparison between the two profiles instead of comparing the peak power continuous discharge with the intermittent. However, this method does not give an exact understanding of the battery behaviour in real scenarios as the current required by a wearable sensor device to perform its operations remain constant, whereas in constant power discharge the current needs to increase as the voltage decreases from the depleting battery. Also, as there is no supply voltage stabilisation mechanism in many sensor devices, the current used decreases with the decline in voltage [17].

This paper focusses on small batteries and uses current consumption profiles indicative of wearable sensors and healthcare devices. The primary purpose of the battery energy is the exchange of data

doi: 10.1049/joe.2017.0303
This is an open access article published by the IET under the Creative Commons Attribution License (http://creativecommons.org/licenses/by/3.0/)

Table 2 Details of the batteries used in this present paper

Battery type	Rechargeable	Open-circuit voltage, V	Cut-off voltage, V	Capacity, mAh	Dimensions ($L \times W$), mm
alkaline	no	1.5	0.9	1500	44.5 × 10.5
Li-ion	no	3.6	0.9	120	24.5 × 5.0
Li polymer	yes	3.7	3.1	110	25.0 × 15.0
Ni–MH	yes	1.2	0.9	1300	50.5 × 14.5

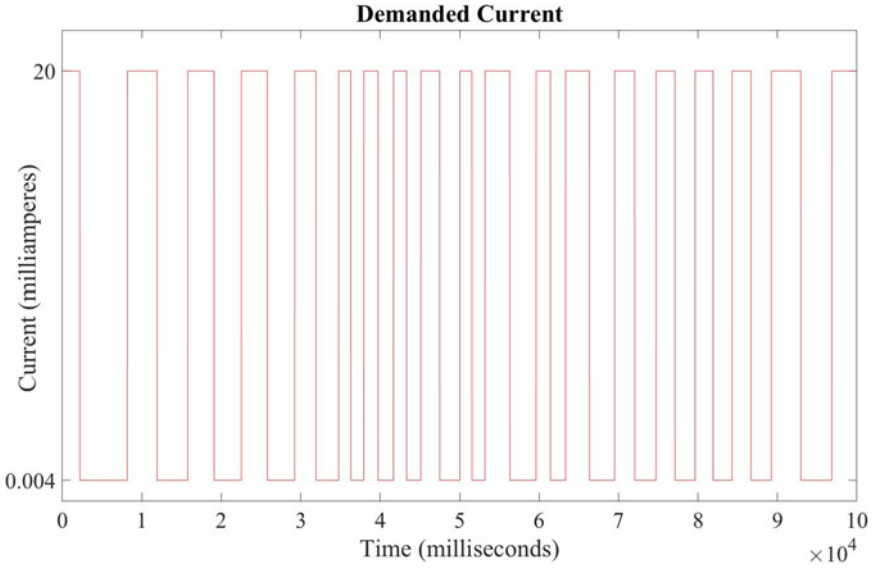

Fig. 2 *Intermittent current demanded during the experiments*

with other wireless hubs/routers such as a cell phone or a smart-home infrastructure.

Thus to have a clear understanding of the battery behaviour in actual scenarios, the constant-current discharge has been used for the present paper. To effectively compare the intermittent discharge pattern with the continuous discharge pattern, the increase in the active time and the total charge delivered by the battery in both scenarios have been considered as these parameters give a better realisation of battery performance under different discharge conditions. In addition, the current values chosen for the experiments correspond to the requirements of a typical wearable device. Since no research has yet been carried out with this perspective, this novel paper will prove insightful to future studies that aim to prolong the operating time of a wearable device by managing the energy available in its power source.

6 Experimental setup

This section presents the details of the experimental setup used to verify the presence of the recovery effect and amount of recovery that is possible in the scenarios compatible with wearable sensors and healthcare devices using typical chemistries.

In the case of rechargeable batteries (Li polymer and Ni–MH), each battery was fully charged to its own specification. In the case of non-rechargeable batteries (alkaline and Li-ion), each battery was new. Each battery was put to discharge through a constant-current discharge circuit which drains the battery current via specified current values for active and sleep modes. The battery voltage was recorded at a sampling rate of 2 kHz from a randomly varying active/sleep profile as discussed below.

6.1 Batteries used

The most commonly used battery chemistries in typical wearable devices have been tested for their behaviour. All of the batteries are off the shelf and are easily available. The shape, size and weight of the batteries are in alignment with typical requirements of wearable devices. Table 2 presents the relevant details of the batteries used in the experiments.

6.2 Discharge pattern

A number of different discharge patterns were created by varying: (i) discharge current (between active and sleep), (ii) rate of duty cycling, i.e. the ratio of sleep time (S) to active time (A) and (iii) the duration of the active time. The duration of the active time was generated randomly at each discharge time between the ranges of 10 and –60 s. Each active cycle was followed by a sleep cycle with the duration of a sleep cycle determining the rate of duty cycling. A continuous discharge with sleep time $S=0$ (i.e. always active so no recovery occurs), and intermittent discharges of $S=A$ (termed 50%) and $S=2A$ (termed 67%) have been considered for this work. Fig. 2 shows a 100 s snippet of an intermittent current demanded during the experiments.

6.3 Constant-current discharge circuit

Since the terminal voltage of a battery decays with discharge, a constant-current discharge circuit was required for this paper that was able to draw current from non-discharged batteries irrespective of their terminal voltage. A novel design constraint of this system was to switch between active and sleep currents, rather than active and no current, as previously discussed in Section 4, thus emulating the sleep current drain from typical wearable devices. Fig. 3 depicts the circuit diagram of the discharge circuit. A microprocessor controls the active/sleep timings, and has an internal analogue-to-digital converter (ADC) for sampling the analogue voltages and logging to a file. As can be seen in Fig. 2, the length of the active time is random, followed with a sleep time that maintains the active/sleep ratio. The discharge circuit was set to discharge 20 mA

This is an open access article published by the IET under the Creative Commons Attribution License (http://creativecommons.org/licenses/by/3.0/)

doi: 10.1049/joe.2017.0303

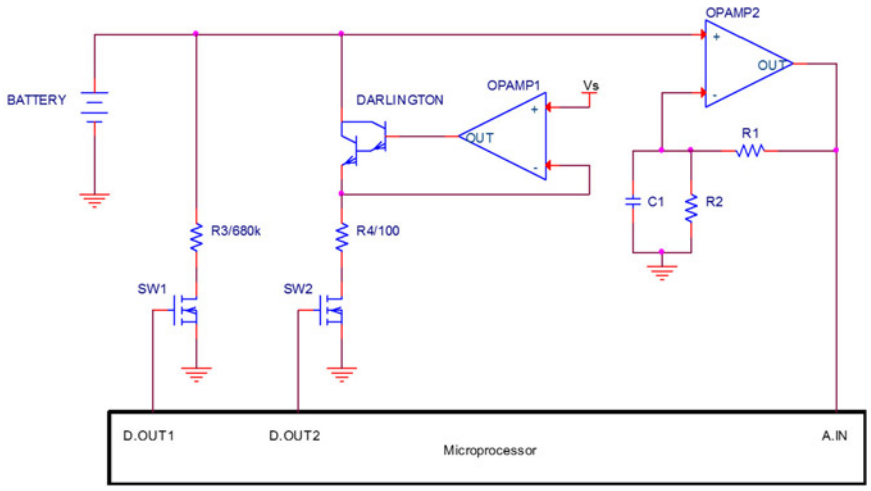

Fig. 3 *Circuit diagram of the constant-current discharge circuit used in the battery discharge measurement system incorporating active and sleep current drains*

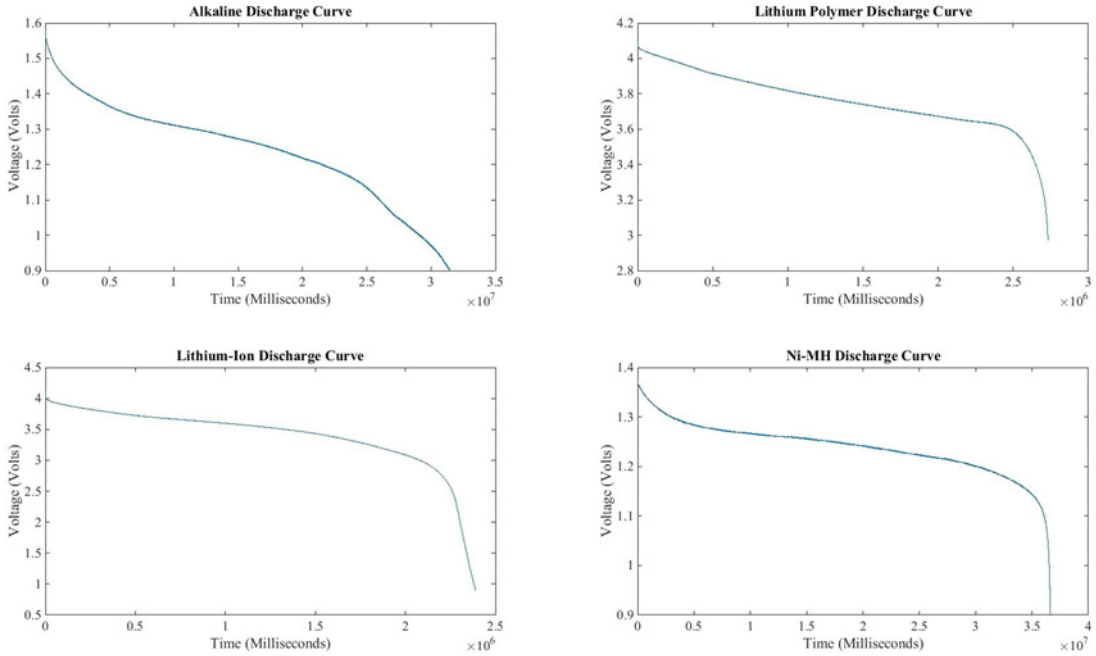

Fig. 4 *Discharge curves of alkaline, Li polymer, Li-ion and Ni–MH batteries obtained from the experimental data*

in the active duration and 4 μA in the sleep duration. This broad range of values covers the range of all the typical current requirements of wearable devices and even other sensor devices [18].

Considering that a typical 100 mAh battery would last 3 years when discharging 4 μA sleep current, then practically the battery self-discharge will mean a shorter useful life. Therefore, the importance of controlling the exact amount of sleep current is less important. Resistor R3 sets the battery current drain in sleep mode [through metal–oxide–semiconductor field-effect transistor (MOSFET) SW1 controlled by microprocessor digital output D.OUT1] defining the sleep period discharge.

To model the current in the active mode, Vs sets the discharge current in the active mode, [1..20] mA. As most power control circuits in wearable devices use DC/DC converters, their current draw is largely independent of supply voltage. The Darlington BJT, OPAMP1 and R4 form a constant-current drain circuit (through MOSFET SW2 controlled by microprocessor digital output D.OUT2) defining the active period discharge. The current drawn from the battery is closely approximated by Vs/R4. In practise, a small amount of base current must flow and hence the choice of Darlington transistor with typical H_{FE} of $\gg$1000. The resulting error is <0.1%.

OPAMP2 forms a high-impedance voltage follower (buffer) to monitor the instantaneous battery voltage, with gain set by 1 + (R1/R2) in order to correctly drive the microprocessor internal ADC pin A.IN. The buffered battery voltage is sampled by the microprocessor at 2 kHz. The high sampling rate allows for capturing the highly dynamic terminal voltages that are of key importance to establish a functional battery model. Low-pass filtering of 100 kHz is provided by C1/R2 for electromagnetic compatibility considerations.

7 Results

The results from this set of experiments are as follows. The overall battery discharge curves were considered as shown in Fig. 4 to estimate the total time for which the battery lasts before reaching the cut-off voltage when the battery no longer has enough terminal

This is an open access article published by the IET under the Creative Commons Attribution License (http://creativecommons.org/licenses/by/3.0/)

voltage to drive the wearable device. Then, for each run, the following parameters were calculated:

(i) *Total active time:* The total time during which the current demanded and delivered was 20 mA (high-current value).
(ii) *Total charge delivered:* The overall charge delivered by the battery during both high- and low-current discharge periods as calculated using the Coulomb counting algorithm [19]. According to this method, the total current drawn is integrated over the total functioning time of the battery.

Table 3 shows the percentage increase achieved in the total active time and the charge delivered when batteries were put to discharge with 50% ($S=A$) and 67% ($S=2A$) duty cycling rate in comparison with when no sleep time was allowed. Also, the mean and standard deviation of these parameters were calculated for multiple runs of each discharge pattern for every battery as detailed in Table 4.

Table 3 Percentage increase in active time and percentage increase in the total charge delivered by the batteries under two duty cycling rates, $S=A$ and $S=2A$

Battery chemistry	Percentage increase in active time		Percentage increase in AC	
	$S=A$	$S=2A$	$S=A$	$S=2A$
alkaline	1.86	*21.3*	1.88	*21.35*
Li polymer	8.55	*11.68*	8.57	*11.87*
Li-ion	1.41	0.74	1.39	0.67
Ni–MH	−3.93	−2.56	−3.91	−2.55

Results in italic text show where there is a significant improvement in effective discharge time, i.e. recovery effect.

The experimental measurement results were further analysed to understand the battery behaviour during the sleep cycles including the voltage rise time. The recovery response during the sleep cycles were examined and modelled using the curve fitting toolbox in MATLAB. It was observed that all curves fit well to (1), being two cascaded first-order responses. Each response has its own gains, a and c, and its own time constants b and d, and f being the average amplitude. The R-square for these fittings was >0.75, demonstrating good curve fitting performance. Fig. 5 shows voltage curve fitting during sleep cycles for each battery

$$v_{\text{out}} = a\left(1-\exp^{-t/b}\right) + c\left(1-\exp^{-t/d}\right) + f \tag{1}$$

The time constants from each of the fittings for both 50 and 67% discharge pattern were obtained. These values have been represented as histograms in Fig. 6 to show the variation in their values during the entire discharge. It can be seen that though most of the values lie in a similar range, a few cases with high values of time constants for 67% discharge were seen. This slight variation observed can be attributed to the limitations of the fitting algorithm since it tends to find local best-fit values instead of the global. Hence, the median was taken for the time constant values and the results are presented in Table 5.

Table 4 Mean values for the batteries when subjected to 0, 50 and 67% discharge rates

Battery chemistry	Extracted charge, mAh			Total active time, s		
	0%	50%	67%	0%	50%	67%
alkaline	*1397.978*	*1424.264*	*1696.549*	*251630.66*	*256314.31*	*305378.92*
Li polymer	*109.143*	*118.501*	*122.19*	*19645.8*	*21326.2*	*21985.42*
Li-ion	137.72	139.672	138.741	24790.13	25,136.61	24,958
Ni–MH	1626.56	1625.38	1627.68	292782.04	292507.88	292982.92

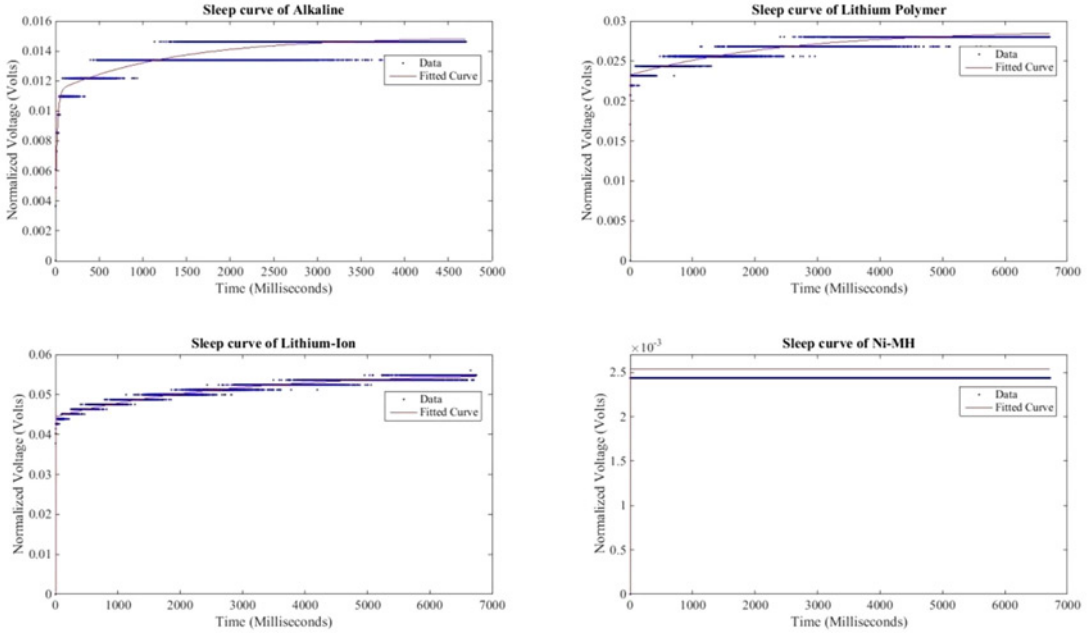

Fig. 5 *Voltage curves during sleep cycle for alkaline, Li polymer, Li-ion and Ni–MH batteries*

This is an open access article published by the IET under the Creative Commons Attribution License (http://creativecommons.org/licenses/by/3.0/)

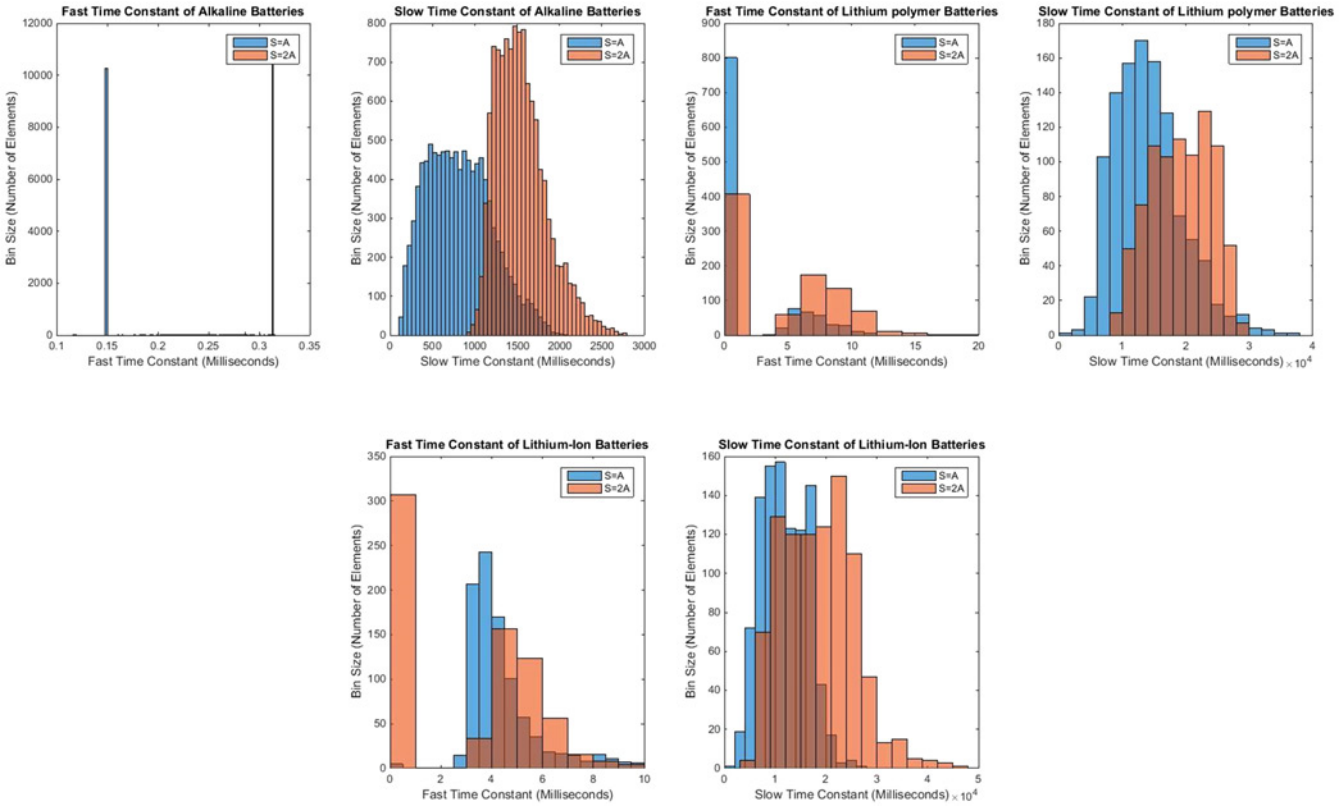

Fig. 6 *Histograms showing the variation in the measured time constants over the full discharge cycle using 50% (S = A) and 67% (S = 2A) for the alkaline, Li polymer and Li-ion batteries. As can be seen, while the actual time constants of the recovery response do very good over the full discharge period, their response times are within two discrete classifications*

Table 5 Average value of slow and fast time constants for both the discharge patterns for all the batteries

Battery chemistry	Fast time constant, ms		Slow time constant, ms	
	50%	67%	50%	67%
alkaline	0.2154	0.3006	1098.6	1848.1
Li polymer	5.7148	9.744	19,264	18,696
Li-ion	5.08	4.98	14,326	25,559

8 Discussion

8.1 Effect of the rest time duration

The duration of rest time plays a critical role in determining the time for which the battery will be capable of delivering the demanded active current and hence the amount of charge that it will be able to deliver. It can be realised from Table 3 that when sleep time equals the active time (i.e. with 50% duty cycling) only a slight increase in the active time and the charge delivered is observed. For both alkaline and Li-ion batteries, there is almost 1.8% increase in the observed active time and the charge delivered. Li polymer batteries have shown a rise of 3.4% for both factors. However, a decrease of almost 3.9% has been observed for Ni–MH batteries. When the sleep time was increased to twice that of the active time, ~21% increase was noted for both parameters in case of alkaline batteries, while Li polymer showed a rise of 9%. Li-ion presented >1% increase, whereas Ni–MH showed a decline in both the amount of charge delivered and the active time. Furthermore, whilst the terminal voltage of Li-ion rises during sleep periods, it did not actually recover charge. Thus it can be inferred that only *alkaline* and *Li polymer* batteries have a tendency to recover significant charge during sleep periods and the amount of gain achieved increases with the increase in the duration of the sleep interval.

8.2 Analysis of voltage curves

The voltage curves for the entire discharge and during every sleep cycle of the batteries have been analysed.

8.2.1 Overall discharge curve: The overall discharge curves are shown in Fig. 4. A typical battery discharge curve generally comprises of an initial exponential discharge period followed by a long normalised duration before it reaches the knee and subsequently hits the cut-off voltage. Different batteries vary in their discharge shapes due to the difference in the inherent chemical species and their rate of reaction. Alkaline and Ni–MH batteries have a prominent initial exponential period as compared with Li-ion and Li polymer batteries which have more of a flatter start. This suggests that the initial voltage variation is higher in alkaline and Ni–MH. The normalised discharge period at the middle of the discharge is very flat for Li-ion followed by Li polymer and Ni–MH batteries in contrast to alkaline batteries for which it is continuously decreasing. The knee portion toward the end of the discharge is much more clearly visible in Li polymer, Li-ion and Ni–MH batteries in comparison with alkaline.

8.2.2 Voltage curves during sleep period: The shape of a voltage curve during a sleep interval is useful in understanding the voltage relaxation process. Fig. 5 presents the voltage curve for all the batteries during sleep cycles from the middle of a discharge cycle. It can be seen that the Ni–MH batteries have flatter curves, i.e. they instantly respond to the step input. However, the other three batteries have significantly visible rise times. The very small time constant of alkaline batteries allows them to rise quickly

doi: 10.1049/joe.2017.0303
This is an open access article published by the IET under the Creative Commons Attribution License (http://creativecommons.org/licenses/by/3.0/)

from the lower voltage and reach the steady state rapidly. On the other hand, Li-ion and Li polymer batteries have similar shapes attributing to the similar range of time constant values.

8.3 Effect on the rise time during sleep cycles

Once the voltage charge/discharge curves were obtained, followed by the realisation of two time constants buried in the recovery curves, research was performed to find a suitable model for the system.

Randles [20] considered electrode reactions, and proposed adding a series tank circuit to the existing battery models that only used a voltage source with a series electrolyte resistance. The tank circuit described the battery dynamics and was formed with the electrode surface capacity in parallel with a series resistance–capacitance circuit modelling the electrode reaction. While it was typical to model the battery discharge with an increasing electrolyte resistance, thus lowering the terminal voltage, Randles' tank circuit was the first to model dynamic electrolyte reaction. However, Randles model was found not to be a good match for the embedded recovery effect of two time constants in this work.

This work found that the battery sleep period satisfies two first-order systems in series (1) and was found to be best modelled by the interactive two-tank system [21]. The kinetic battery model [22] has been used to model the batteries as shown in Fig. 7. The first tank is termed the bounded charge well (BCW) and the second is termed the available CW (ACW). The ACW is responsible for providing charge to the external load, whereas the BCW supplies charge to the ACW. During an active cycle, most of the active species are consumed from the well nearer to the outlet of the ACW. When a sleep period is provided after an active cycle, the active species in the ACW settle toward the well nearer to the outlet, reaching an equilibrium state. During this time there is also a flow of species from the BCW toward the ACW. The number of species that move across and their speed is proportional to the time constant values. A small time constant indicates the faster movement of active species, whereas a larger value indicates a slow movement, and therefore two time constants. Hence, to achieve a higher utilisation of the battery's chemical material for an increase in the overall charge delivered, the smaller time constant values are essential. Equation (1) was used for modelling the voltage curves during sleep cycles and indicated the presence of two time constants. One is a slow time constant which primarily governs the movement of species from the bounded to the ACW, whilst the fast time constant relates to the alignment in the ACW toward the outlet.

Table 5 summarises the time constant values for all three batteries. It can be seen that alkaline batteries have the smallest value of fast and slow time constants in comparison with the other two batteries which have higher and similar range of values. This implies that alkaline batteries have faster movement and settlement of the species, thus they require small sleep durations to recover charge delivered, whereas the higher value of time constants in Li polymer suggest slower movement of the species leading to the requirement of comparatively longer sleep intervals to recover charge.

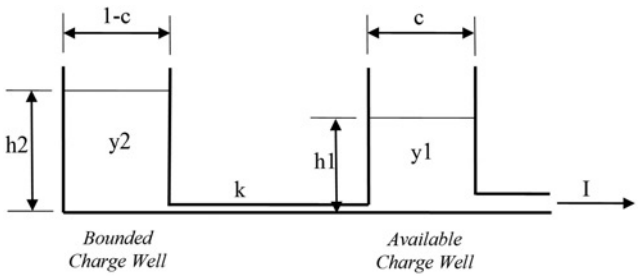

Fig. 7 *Battery modelling as two CWs of kinetic battery model [22]. The slow time constant is represented by the left-hand well with a narrow channel to the right-hand well. The fast time constant is represented by the right-hand well supplying the exit channel*

9 Conclusions

This paper has presented experimental results conducted in order to validate the presence of recovery effect in commonly used off-the-shelf batteries in wearable sensors and healthcare devices. Alkaline, Ni–MH, Li-ion and Li polymer batteries were tested for their behaviour under pulsed discharge conditions with duty cycling discharge rates of 50 and 67%. While the literature has investigated the recovery effect using active and off periods of time, the novelty of our results is that when we discharge the batteries to see the recovery effect, we include a small drain current to model the typical sleep current drawn from wearable devices. The total charge delivered and the total active time were analysed for each of these scenarios and compared with the values obtained with the continuous discharge, in order to determine the charge gain that can be achieved from one charge cycle of the rechargeable battery or one use of the non-rechargeable battery. It was observed that alkaline batteries show a significant amount of AC gain and hence active time when subjected to intermittent discharge conditions. Almost 21% rise was observed for both parameters with 67% duty cycling rate. In the case of Li polymer batteries, an increase of 11% was obtained when batteries were allowed to sleep for twice the time they were active while the rise was 8.5% when sleep time was equal to active. On the other hand, a marginal gain of only around 1% was observed for Li-ion batteries in both types of pulsed discharge profiles emphasising that Li-ion batteries do not exhibit the recovery effect. Furthermore, in the case of Ni–MH batteries, instead of observing any gain a drop of 3–4% in the charge delivered over the active time was observed. These findings emphasise that the recovery effect does not depend on the recharge capabilities of a battery but rather it is dependent on its chemical composition.

The novel contribution of this work was to find that the recovery effect discharge curve profiles could be accurately modelled using two time constants. Each recovery curve contained slow and fast time constants. These values represent the rate of movement of active species inside the battery. The smaller values indicate faster movement and hence faster recovery of the charge. Alkaline batteries have the smaller time constant values in comparison with Li polymer batteries and are thus capable of recovering charge much faster and in shorter sleep cycles. To incorporate the two time constants seen from this work, it is proposed that the recovery effect is best modelled using a two-tank model constructed of two first-order systems in series which has good match to the practical batteries tested.

From all these findings, it can be deduced that the recovery effect does indeed exist and owes its existence largely to the active material present. This process leads to significant amounts of gain in the total charge that can be extracted out of the battery when the battery is allowed to relax in discharge, hence making it desirable for use in applications where re-charging and replacement are difficult. This work has increased the AC for battery-powered devices between 11 and 21%. When considering the typical operation time on one charge and the operating current for modern wearable devices, then the time between charging for a wearable device can be extended by several days using these results.

10 Future work

The recovery effect needs to be explored further to determine the maximum duration of the active cycle that can be allowed before a battery should switch to sleep mode in order for the recovery effect to fully occur. This would prove beneficial for applications/

This is an open access article published by the IET under the Creative Commons Attribution License (http://creativecommons.org/licenses/by/3.0/)

scenarios that cannot afford longer sleep intervals but could accommodate shorter ones. Also, it would be interesting to analyse if there is any upper bound to the amount of charge recovery that could be obtained from a battery. This would be helpful in avoiding unnecessary long sleep intervals. In addition, other sizes of a battery should also be analysed to compare the percentage effectiveness of different sizes on the active time and charge delivered.

11 Acknowledgments

This work was performed under the SPHERE IRC funded by the UK Engineering and Physical Sciences Research Council (EPSRC), grant EP/K031910/1, and the University of Reading Research Endowment Trust Fund. Sadly, paper author Harneet Arora passed away on the 30th December 2016, just before the final manuscript draft of this paper was completed. The rest of the authors are extremely grateful to the Arora family for permission to submit this work in Harneet's memory.

12 References

[1] Barakah D.M., Ammad-Uddin M.: 'A survey of challenges and applications of wireless body area network (WBAN) and role of a virtual doctor server in existing architecture'. Proc. Third IEEE Int. Conf. Intelligent Systems Modeling and Simulation, Kota Kinabalu, Malaysia, February 2012, pp. 214–219, doi: 10.1109/ISMS.2012.108

[2] Chiasserini C.F., Rao R.R.: 'Improving battery performance by using traffic shaping techniques', *IEEE J. Sel. Areas Commun.*, 2001, **19**, (7), pp. 1385–1394, doi: 10.1109/49.932705

[3] Jongerden M.R., Haverkort B.R.: 'Which battery model to use?', *IET Softw.*, 2009, **3**, (6), pp. 445–457, doi: 10.1049/iet-sen.2009.0001

[4] Narayanaswamy S., Schlueter S., Steinhorst S., *ET AL.*: 'On battery recovery effect in wireless sensor nodes', *ACM Trans. Des. Autom. Electron. Syst.*, 2016, **21**, (4), pp. 1–28, doi: 10.1145/2890501

[5] Crompton T.R.: 'Battery reference book' (Newnes, 2000, 3rd edn.)

[6] http://www.batmax.com/technology-degeneration.php, accessed January 2017

[7] http://chem.libretexts.org/Core/Analytical_Chemistry/Electrochemistry/Case_Studies/Rechargeable_Batteries, accessed January 2017

[8] Rakhmatov D., Vrudhula S.B.K.: 'Time-to-failure estimation for batteries in portable electronic systems'. Proc. IEEE Int. Symp. Low Power Electronics and Design, CA, USA, August 2001, pp. 88–91, doi: 10.1109/LPE.2001.945380

[9] Nelson R.F., Rinehart R., Varley S.: 'Ultrafast pulse discharge film and recharge battery capabilities of thin-metal film battery technology'. Proc. 11th IEEE Int. Pulsed Power Conf., Baltimore, USA, June–July 1997, pp. 636–641, doi: 10.1109/PPC.1997.679411

[10] Castillo S., Samala N.K., Manwaring K., *ET AL.*: 'Experimental analysis of batteries under continuous and intermittent operations'. Proc. Int. Conf. Embedded Systems Applications, June 2004, pp. 18–24

[11] Lafollette R.M.: 'Design and performance of high specific power, pulsed discharge, bipolar lead acid batteries'. Proc. Tenth IEEE Battery Conf. Applications and Advances, CA, USA, January 1995, pp. 43–47, doi: 10.1109/BCAA.1995.398511

[12] Fuller T.F., Doyle M., Newman J.: 'Relaxation phenomena in lithium-ion-insertion cells', *J. Electrochem. Soc.*, 1994, **141**, (4), pp. 982–990, doi: 10.1149/1.2054868

[13] Lee Y.S., Sun Y.K., Nahm K.S.: 'Synthesis and characterization of $LiNiO_2$ cathode material prepared by an adiphic acid-assisted sol–gel method for lithium secondary batteries', *Solid State Ion.*, 1999, **118**, (1–2), pp. 159–168, doi: 10.1016/S0167-2738(98)00438-X

[14] Reichert M., Andre D., Rösmann A., *ET AL.*: 'Influence of relaxation time on the lifetime of commercial lithium-ion cells', *J. Power Sources*, 2013, **239**, pp. 45–53, doi: 10.1016/j.jpowsour.2013.03.053

[15] Pei L., Wang T., Lu R., *ET AL.*: 'Development of a voltage relaxation model for rapid open-circuit voltage prediction in lithium-ion batteries', *J. Power Sources*, 2014, **253**, pp. 412–418, doi: 10.1016/j.jpowsour.2013.12.083

[16] Devarakonda L., Hu T.: 'Effects of rest time on discharge response and equivalent circuit model for a lead-acid battery', *J. Power Sources*, 2015, **282**, pp. 19–27, doi: 10.1016/j.jpowsour.2015.02.030

[17] Mikhaylov K., Tervonen J.: 'Optimization of microcontroller hardware parameters for wireless sensor network node power consumption and lifetime improvement'. Proc. IEEE Int. Congress Ultra Modern Telecommunications and Control Systems and Workshops, Moscow, Russia, October 2010, pp. 1150–1156, doi: 10.1109/ICUMT.2010.5676525

[18] Milenković A., Otto C., Jovanov E.: 'Wireless sensor networks for personal health monitoring: issues and an implementation', *J. Comput. Commun.*, 2006, **29**, (13–14), pp. 2521–2533, doi: 10.1016/j.comcom.2006.02.011

[19] Ng K.S., Moo C.S., Chen Y.P., *ET AL.*: 'Enhanced Coulomb counting method for estimating state-of-charge and state-of-health of lithium-ion batteries', *Appl. Energy*, 2009, **86**, (9), pp. 1506–1511, doi: 10.1016/j.apenergy.2008.11.021

[20] Randles J.E.B.: 'Kinetics of rapid electrode reactions', *Discuss. Faraday Soc.*, 1947, **1**, p. 11, doi: 10.1039/df9470100011

[21] Coughanowr D.R., LeBlanc S.E.: 'Process systems analysis control' (McGraw-Hill, 1994, 3rd edn)

[22] Manwell J.F., McGowan J.G.: 'Extension of the kinetic battery model for wind/hybrid power systems'. Proc. Fifth European Wind Energy Association Conf., 1994, pp. 284–289

This is an open access article published by the IET under the Creative Commons Attribution License (http://creativecommons.org/licenses/by/3.0/)